The observation of soil microstructure under load

Y. P. Cheng, D. J. White, E. T. Bowman, M. D. Bolton & K. Soga
Cambridge University Engineering Department

ABSTRACT: This paper describes some new techniques of image analysis, which offer an insight into the micromechanical behaviour of granular media. These techniques have been developed to provide a grain-scale commentary on the highly non-linear macroscopic behaviour of soil under load. The techniques are illustrated by two example applications: an element test and a physical model. Digital photography provides both grain-scale observations of sand particles under changing load and measurements of the resulting macroscopic strain. Image analysis is used to quantify changes in particle shape and fabric anisotropy. The resulting observations provide some explanations of the micromechanical origins of macroscopic properties.

1 INTRODUCTION

Many macroscopic phenomena of granular media are dealt with through element testing or physical modelling. Constitutive models based on simple element tests often have scores of parameters, most of which are the result of curve-fitting, and have no physical significance at grain-scale. It is not known which grain-scale properties are reflected in macroscopic measurements of strength and stiffness.

Reduced-scale models of boundary value problems can be extremely sophisticated, and bypass the designer's need for a constitutive model. However there is often doubt concerning the dependence of the macroscopic behaviour on the grain-scale properties. For self-similarity in physical modelling, what grain-scale properties must be reproduced?

This paper addresses these issues by presenting a number of novel experimental techniques based on high-quality image capture and analysis. These techniques allow grain-scale phenomena to be observed in parallel with macroscopic measurements of continuum behaviour. Two applications are used for illustration; an element test and a physical model.

2 IMAGING TECHNIQUES

2.1 *Close-up digital photography to observe grain-scale behaviour*

Digital still cameras are rapidly decreasing in cost whilst increasing in sophistication. The improved resolution provided by a 2-megapixel CCD compared to conventional video, combined with the use of close-up lenses, allows an inexpensive ($400) digital camera to provide images comparable to those obtained through optical microscopy. This allows an experiment to be observed at grain-scale without deploying a bulky microscope.

2.2 *Standard digital photography combined with Particle Image Velocimetry (PIV)*

PIV is a velocity-measuring technique which is widely used in fluid mechanics and has now been adapted for measuring the flow of soil (White *et al*, 2001). Algorithms have been written which allow the movement of sand to be measured to a precision of 1/15th of a pixel. By summing the incremental displacements through a series of images, the developing strain field can be observed.

2.3 *Image analysis to quantify anisotropy*

Conventional techniques for preparing element test samples and physical models produce soil fabric which is inherently anisotropic. The origin of the anisotropic strength and stiffness of granular materials at a macroscopic level (constitutive anisotropy) is the anisotropic orientation of the grains and grain contacts (fabric anisotropy). Little progress has been made in linking these micro- and macro-phenomena. This could be attributed to two problems.

i. the difficulty in observing soil fabric in situ.
ii. the difficulty in making a quantitative measurement of the soil fabric.

The first problem can be overcome by using resin injection to preserve the soil fabric within an element test whilst the external load is removed and the sample is prepared for Scanning Electron Microscopy (SEM) photography. In the case of a physical model deforming behind an observation window, grain-scale close-up digital photography (section 2.1) can capture the soil fabric in situ.

2.4 *Fourier Descriptor Analysis (FDA)*

Post-test analysis of sand particles after a loading event can quantify the consequential changes in particle size and shape. SEM images are used to obtain the outline shape of the grains. A quantitative assessment of particle shape can then be found by FDA; Bowman *et al* (2000). This technique characterises morphology according to coefficients of Elongation, Triangularity, Squareness and Asymmetry, which are denoted "Signature Descriptors".

3 GRAIN-SCALE AND MACROSCOPIC OBSERVATIONS IN AN ELEMENT TEST

3.1 *A miniature oedometer*

McDowell and Bolton (1998) point out that all compressibility relations involving only the voids ratio and the applied stress are dimensionally inconsistent. They introduce the crushing strength of grains as the normalising factor for plastic compression, and reducing size of fragments as the origin of plastic hardening. The normal compression line (NCL) on a plot of voids ratio versus the logarithm of effective stress is then seen as the expression of fractal self-similarity in the filling of voids through the successive breaking of fragments. In the laboratory, Nakata (1999) has demonstrated how the onset of particle damage at asperities can be linked with the onset of plastic yielding.

Further insights might be gained if microstructure could be viewed continually during a test. A miniature oedometer 10mm in diameter was designed to observe the breakage of 5mm high samples of dry Dog's Bay carbonate sand behind a glass lens during one-dimensional compression (Fig. 1). A calibrated strain gauge on the neck of the apparatus measures the load acting on the sand whilst the piston is slowly advanced. Images of the compressing sand are captured by a Kodak DC280 digital camera with a +40 magnifying lens.

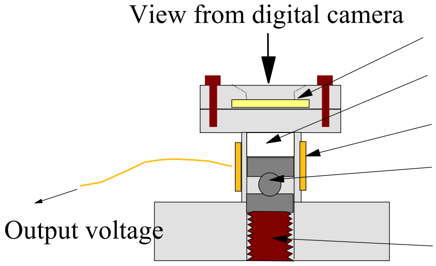

Figure 1. Set-up of miniature oedometer.

3.2 *Macroscopic observations*

The measured stress-volume data from 3 oedometer tests is plotted in Fig. 2. The ultimate slope of the NCL agrees with Golighty (1990).

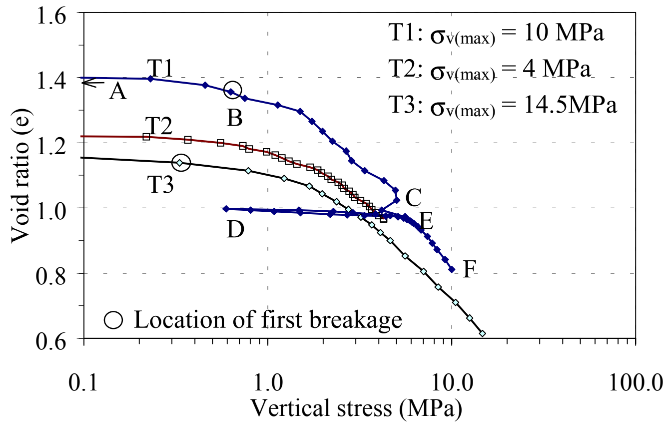

Figure 2. One-dimensional compression curves.

3.3 *Microscopic observations*

Fig. 3 shows images from Test 1. The individual sand grains could be seen clearly at 0 MPa (Fig. 3a). At first the sand grains can be seen to rearrange without breakage. This is associated with the first part of the compression curve, which is conventionally called "elastic" or "recoverable".

a: σ_v=0 MPa b: σ_v=10 MPa

Figure 3. Images of oedometer test (T1) at two stress levels.

First breakage of the sand grains occurred at stress levels of around 0.2-0.6 MPa, which indicates the beginning of irrecoverable strain. This early plastic response was found to be linear in a plot of voids ratio versus stress on a natural scale, consistent with the data of Liu et al. (2000). Pictures of soil microstructure show that this linear plastic response is governed by a combination of three processes: contact damage, continued breakage of specific particles (e.g. Fig. 4, A to F), and breakage of fresh particles in new locations (Fig. 3b) with rearrangement of the broken pieces. By the time the (fractal) NCL has been reached, many large particles have become successively fragmented, and the camera can not resolve the finest pieces (1 pixel = 10 μm).

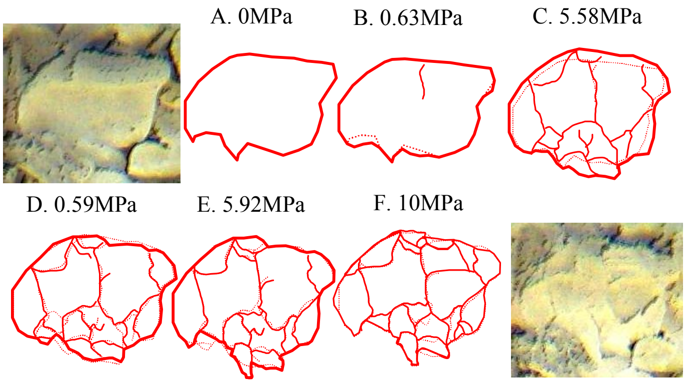

Figure 4. Progressive breakage of a selected grain.

Fig. 4 shows the continuous breakage of a selected sand grain over a macroscopic stress range 0 to 10 MPa with an unload reload loop at 5.58 MPa. The locations of these pictures are indicated (A to F) in the compression curve (Fig. 2). First breakage (at B) occurred at 0.63 MPa. This particular grain did not undergo rearrangement but further breakage was observed up to C when unloading of the sample took place. During unloading (at D), no significant particle rearrangement was observed. When reloading to 5.92 MPa, relative movement of the broken pieces was observed (at E). Further breakage continued as the compression proceeded along the NCL (to F).

4 GRAIN-SCALE AND MACROSCOPIC OBSERVATIONS WITHIN A PHYSICAL MODEL

4.1 *The penetration of a foundation pile*

The strength of piles driven into sand is arguably the topic of greatest uncertainty in foundation design (Randolph *et al*, 1994). There is no accepted consensus of the mechanism by which a pile penetrates soil (i.e. the soil displacement and strain fields).

To address this uncertainty, a plane strain test chamber (1000x650mm) with a transparent window has been constructed. A model pile is pushed into the chamber whilst the resulting soil displacement is captured by digital photography. The image analysis techniques developed for this experiment are illustrated here using some data from a test on loose Dog's Bay carbonate sand (e_o = 1.48). The load on the tip of the pile remained steady at 2.1 MPa during penetration. Three 4mm x 4mm elements of soil which are located at differing positions around the pile have been chosen for examination.

4.2 *Macroscopic observations*

Digital photography combined with PIV image analysis (White *et al*, 2001) allows the strain paths of soil elements A, B and C to be found. Noting that significant rotation occurs, a strain algorithm which separates shear strain from rigid body rotation has been used. During penetration, elements A, B and C rotate by 17, 29, and 2 degrees respectively.

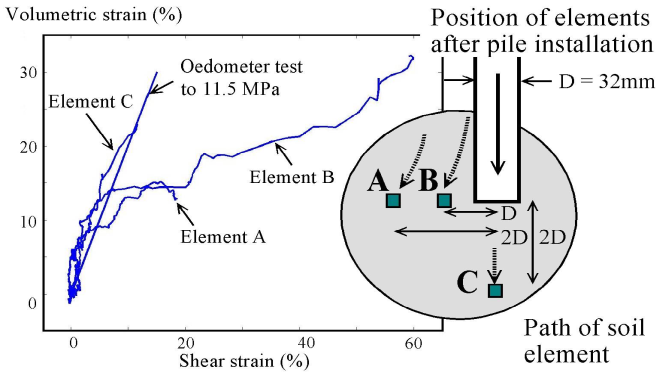

Figure 5. Strain paths of elements close to pile.

The element paths in shear strain - volumetric strain space are shown in figure 5, permitting convenient comparison with element test results. The strain path of an oedometer test with similar initial voids ratio (e_o = 1.49) is superimposed. A key observation is that the combination of high shear strain, and relatively low but rotating applied stresses (σ_{max} ≈ 2.1 MPa) on element B, induces a comparable volumetric strain to one-dimensional compression up to 11.5 MPa, about 5 times larger.

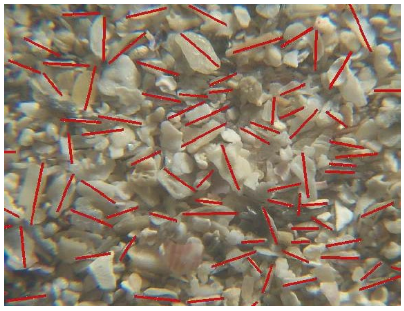

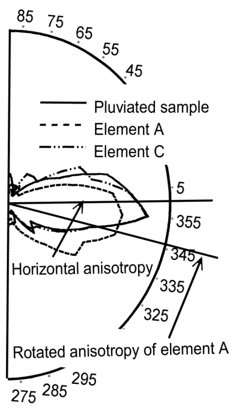

Above: pluviated sample
Right: Angular distribution of particle major axes

Figure 6. Fabric anisotropy of soil elements.

4.3 *Microscopic observations*

Figure 6 shows a zone of pluviated soil prior to pile penetration, with the major particle axes marked. The chart of major axis distribution shows a distinct concentration of major axes oriented horizontally. This indicates that pluviation of the elongated Dog's Bay sand particles produces a strongly anisotropic fabric. Examination of elements A and C shows similarly anisotropic fabric. It is interesting to note that the 17° rigid body rotation of soil element A captured by the PIV analysis is partly reflected in the 14° rotation of the plane of anisotropy. Any difference in the measured rigid body rotation and the observed fabric rotation is evidence that induced stresses have reoriented the soil fabric.

5 COMPARATIVE MICROSCOPIC OBSERVATIONS

5.1 *Grain size*

Particle size distributions of the element tests (Fig. 7) show that all the original 25% by mass of largest particles (> 800 μm) were broken and 28% of fine particles (< 300 μm) was found after the sand was compressed to the NCL (T3), which is consistent with the observations in section 3.3. These fines are the broken edges of the medium or large particles.

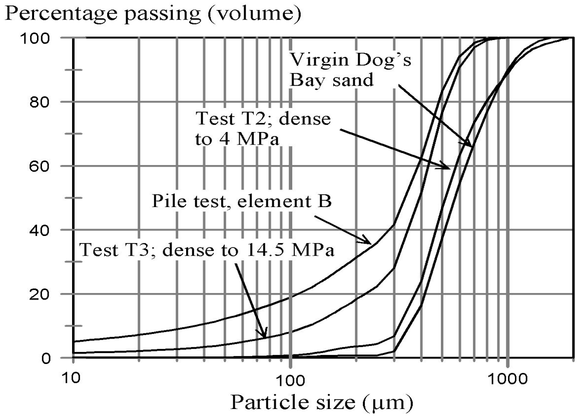

Figure 7. Grading curves of virgin and tested sands.

The particle size distribution curve of model element B is also shown. This result mirrors the disparity described in section 4.2. Significantly greater particle breakage has occurred around the pile than in the oedometer, showing that both high shear strains and high stress levels drive particle breakage.

5.2 *Grain shape*

FDA allows quantification of the evolving particle morphology via different crushing processes. Fig. 8 shows the mean Signature Descriptor coefficient, normalised against the virgin soil, for particles of various radii. Fig. 8a is taken from pile element B and Fig. 8b is from a mini-oedometer test similar to T3. Despite the different gradings of the two tests, the development of particle shape by crushing is very similar. In both cases, crushing produces more rounded particles in the large size range, with Elongation less than 60% and Triangularity approximately 90% of the virgin soil. Smaller particle fragments are more elongated and triangular. However, comparing the relative changes, the soil in Fig. 8b may be considered to be at an earlier stage of breakage than the soil in Fig. 8a which has fewer large particles and a greater number of small flakes even though its stress level was smaller. Asymmetry is still developing in Fig 8b with the coefficient varying from 85% to 67% of the original, whilst for Fig. 8a it is virtually constant at 69% - implying that the soil has reached a self-similar plateau. The trend of Squareness differs between the two processes, which may be a function of the relative shearing, though further analysis is required to investigate this.

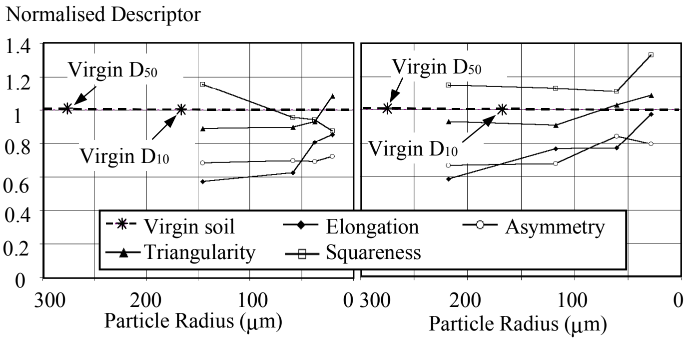

a. Pile test, element B b. Dense sand, 10 MPa

Fig. 8. Signature Descriptors of virgin and tested sands.

6 CONCLUSIONS

Inexpensive digital cameras have provided continuous microscopic evidence of the crushing and rearrangement of soil grains in element and model tests. Plastic soil behaviour is seen to be related to grain crushing, which is depends both on stress level and on the magnitude of shear strain.

The same images simultaneously provide macroscopic data of displacement fields and their derivatives – volumetric and shear strain, and fabric rotation. Conventional element tests conducted up to about 20% strain would not approach the deformations produced by pile driving.

Particle size analyses offer a post-test measure of grain crushing from a sample recovered from the soil body. Issues of sampling, especially in relation to the significance of images sampled through a window, deserve much greater attention.

REFERENCES

Bowman, E.T., Soga, K. & Drummond, T.W. 2000. *Particle shape characterisation using Fourier analysis.* Technical report CUED/D-SOILS/TR315, Cambridge University.

Liu, M.D., Carter, J. & Hull, T.S. 2000. *Compression behaviour of sands.* Research Report R801. Syndey University.

Golighty, C.R. 1990. *Engineering properties of carbonate sands.* Bradford University. Ph.D. thesis.

McDowell G.R. & Bolton M.D. 1998. On the micromechanics of crushable aggregates. *Geotechnique* 48 (5): 667-679.

Nakata Y., Hyde A.F.L. & Murata H. 1999. A probabilistic approach to sand particle crushing in the triaxial test. *Geotechnique* 49 (5): 567-538.

Randolph, M.F., Dolwin, J. & Beck, R. 1994. Design of driven piles in sand. *Geoptechnique* 44 (3): 427-448.

White, D.J., Take, W.A. & Bolton, M.D. 2001. Measuring soil deformation in geotechnical models using digital images and PIV analysis. *Proc. 10th IACMAG Conference*, Tucson, Arizona.